Deep-Sea Research Part I 139 (2018) 104–113

Contents lists available at ScienceDirect

Deep-Sea Research Part I

journal homepage: www.elsevier.com/locate/dsri

On the translation of Agulhas rings to the western South Atlantic Ocean

Luiz Alexandre A. Guerra[a,b,*], Afonso M. Paiva[a], Eric P. Chassignet[c]

[a] Programa de Engenharia Oceânica - PEnO/COPPE, Universidade Federal do Rio de Janeiro (UFRJ), Centro de Tecnologia, Bl. C - Sala 203, Caixa Postal 68508, Cidade Universitária, Rio de Janeiro, RJ 21949-900, Brazil
[b] PETROBRAS/CENPES, Av. Horácio Macedo, 950 - Cidade Universitária, Rio de Janeiro, RJ 21941-915, Brazil
[c] Center for Ocean-Atmospheric Prediction Studies (COAPS), Florida State University, 2000 Levy Avenue, Tallahassee, FL 32306-2840, USA

ARTICLE INFO

Keywords:
Agulhas rings
Eddy detection
South Atlantic Ocean
Brazil Current

ABSTRACT

The shedding of Agulhas rings is the primary process connecting the Indian and Atlantic oceans. The rings transport warm and salty waters that feed the surface limb of the Atlantic Meridional Overturning Circulation. Early studies suggest that Agulhas rings decay and diffuse their contents within the South Atlantic subtropical gyre. In this paper, we update the ring census using an automated algorithm to detect and track eddies over more than 23 years of satellite altimetry data (1993–2016) and calculate their main characteristics. While 140 rings spawned from the Agulhas Retroflection, their following splitting and merging resulted in 74 long-lived rings that crossed the Walvis Ridge and translated towards the west. Eventually, three rings reached the western boundary. For one of them, we use *in situ* measurements to document its interaction with the Brazil Current and two cyclonic eddies, which resulted in a current velocity increase by three times. Although already hypothesized, this interaction had not been demonstrated with *in situ* evidence until now.

1. Introduction

The heat flux towards the equator makes the South Atlantic unique among the other oceans (Bennett, 1978; Hastenrath, 1982). One of the reasons for such flux is the warm inflow at its southeastern corner provided by the leakage of Indian Ocean water through the Agulhas Retroflection. This warm water primarily feeds the surface route of the Atlantic Meridional Overturning Circulation (AMOC), which eventually returns to the North Atlantic to compensate the production and export of North Atlantic Deep Water (NADW) (Gordon, 1986; Gordon et al., 1992).

The Agulhas Retroflection regulates the heat and salt transfer between the Indian and Atlantic oceans playing a key role in the global climate system (de Ruijter et al., 1999; Matano and Beier, 2003). It is formed when the Agulhas Current, the western boundary current that closes the subtropical gyre in the South Indian Ocean, flowing southwestward along the Southeast African coast until the southernmost tip, detaches and bends upon itself in a tight anticlockwise curve back to the Indian Ocean. Part of Agulhas Current then makes its way into the Atlantic through filaments, direct leakage, and ring shedding (Bang, 1970; Gordon, 1985, 1986; Lutjeharms and Van Ballegooyen, 1988a; Lutjeharms and Cooper, 1996). The retroflection may be shifted westward or eastward according to the zero wind stress curl latitude and the magnitude of the Agulhas Current transport. In response, the Agulhas leakage may increase or almost cease with impact on the thermohaline circulation on a global scale and hence on the earth's climate, as revealed by paleo records (de Ruijter and Boudra, 1985; Lutjeharms and Van Ballegooyen, 1988b; Biastoch et al., 2009; van Sebille et al., 2009; Beal et al., 2011; Nof et al., 2011). However, investigations have been contradictory in their conclusion on whether the leakage has shown an upward trend or no trend over the past decades (Biastoch et al., 2009; Beal et al., 2011; Garzoli et al., 2013; Le Bars et al., 2014).

The majority of the transfer of tropical and subtropical water masses from the South Indian Ocean to the South Atlantic occurs through the shedding of Agulhas rings at the retroflection (Gordon, 1986; Lutjeharms, 1996; de Ruijter et al., 1999). Juvenile Agulhas rings are large anticyclonic eddies with a mean diameter of 242 ± 38 km (Duncombe Rae, 1991) and depths that can reach 4.5 km (van Aken et al., 2003). There is no apparent periodicity on shedding events (Goni et al., 1997), and rings are formed on average every two months (van Ballegooyen et al., 1994; Lutjeharms, 1996; Dencausse et al., 2010). The warm and salty waters conveyed from the Indian Ocean contribute to increased evaporation rates in the South Atlantic and affect the AMOC (de Ruijter et al., 1999; Weijer et al., 2002; Beal et al., 2011). According to Casanova-Masjoan et al. (2017), due to a decay time of approximately 1 year, most of the property anomalies contained within the rings will be diffused into the South Atlantic subtropical gyre and hence advected to the north through the AMOC. The ratio between the

* Corresponding author at: PETROBRAS/CENPES, Av. Horácio Macedo, 950 – Cidade Universitária, Rio de Janeiro, RJ 21941-915, Brazil.
E-mail address: laguerra@petrobras.com.br (L.A.A. Guerra).

https://doi.org/10.1016/j.dsr.2018.08.005
Received 6 January 2018; Received in revised form 24 May 2018; Accepted 7 August 2018
Available online 16 August 2018
0967-0637/

fluxes of warm and salty water from the leakage and the cooler and low-salinity water from the Drake Passage defines the thermocline characteristics of the South Atlantic (Gordon and Haxby, 1990; Gordon et al., 1992). Considering waters warmer than 10 °C, the flux of Indian Ocean water into the Atlantic by Agulhas rings is estimated at 6.3 Sv (1 Sv = 10^6 m^3/s), and the fluxes of heat and salt at 0.045 PW and 78 Pg/year, respectively (van Ballegooyen et al., 1994). To put these numbers in perspective, the total meridional heat at mid-latitudes in the South Atlantic has been estimated as + 0.43 ± 0.08 PW (McDonagh and King, 2005), and the volume transport of the AMOC as ~11 Sv (Wunsch and Heimbach, 2013).

Just after shedding, the Agulhas rings present a distinct warm circular signature at the surface (Lutjeharms and Gordon, 1987) that is erased within a few weeks by intense heat exchange with the cooler atmosphere and mixing due to wind stress (Mey et al., 1990; Olson et al., 1992). Despite losing their surface thermal signature, the rings maintain a positive sea level anomaly (SLA) which can be tracked by satellite altimetry while translating westward across the South Atlantic Ocean (Fu and Zlotnicki, 1989; Gordon and Haxby, 1990; van Ballegooyen et al., 1994; Byrne et al., 1995; Gründlingh, 1995; Witter and Gordon, 1999; Schouten et al., 2000).

In the Cape Basin, the Agulhas rings move northwestward embedded in the Benguela Current creating an eddy corridor to the Walvis Ridge (Garzoli and Gordon, 1996; Goni et al., 1997). This ridge constitutes an obstacle to the translation of deep-reaching eddies into the Atlantic as they usually show a deflection of trajectory and reduction of drift speed while they manage to pass through the deepest valleys (Olson and Evans, 1986; Gordon and Haxby, 1990; Byrne et al., 1995; Arhan et al., 1999). Modeling studies reveal that baroclinic eddies can cross the ridge while the barotropic or near-barotropic cannot (Kamenkovich et al., 1996; Beismann et al., 1999; Matano and Beier, 2003). Early investigations of the period between 1993 and 1996 showed that about two-thirds of the Agulhas rings left the Cape Basin, traveling westward at speeds of 5–8 cm/s between 25°S and 35°S (Gordon and Haxby, 1990; Schouten et al., 2000).

The increase in surface water salinity due to evaporation and the wind forced mixing converts the Indian Ocean water brought to the Cape Basin into South Atlantic typical water (Gordon and Haxby, 1990; Olson et al., 1992). Nevertheless, thermostads and halostads with water characteristics from the Indian Ocean have been identified within rings both in the Cape Basin and west of the Walvis Ridge (McCartney and Woodgate-Jones, 1991; Byrne et al., 1995; Garzoli et al., 1999). This fact indicates that below the surface part of their original thermohaline characteristics may be preserved during translation into the South Atlantic Ocean.

The Agulhas rings are among the largest and most energetic eddies in the world's ocean. The energy contribution of a single ring is equivalent to 7% of the annual wind energy influx over the South Atlantic basin between 10°S and 45°S (Olson and Evans, 1986). Their propagation across the South Atlantic Ocean drives significant interannual variability in the upper layer transport at the northern branch of the subtropical gyre (over 2 Sv RMS for a mean flow on the order of 10 Sv) (Garnier et al., 2003).

In early studies, Geosat SLA maps were used to track Agulhas rings for long distances far from the retroflection region (Gordon and Haxby, 1990; Byrne et al., 1995). However, it is only after the TOPEX/Poseidon mission, that a sufficiently long time-series was produced to permit the tracking of an Agulhas ring from its formation site until 38°W (Schouten et al., 2000). More recently, automatic tracking algorithms have been used over merged multi-satellite altimetric maps to identify and follow ocean eddies (Chelton et al., 2007, 2011). Long ring trajectories and the analysis of energy decay curves support the hypothesis that Agulhas rings might collide with the Brazil Current and trigger transport anomalies (Gordon and Haxby, 1990; Byrne et al., 1995; Nof, 1999; Azevedo et al., 2012), but no *in situ* evidence has been put forward so far.

In this paper, we present the results of a new census of Agulhas rings performed using an automated hybrid eddy detection algorithm (Halo et al., 2014) on 23 years of merged multi-satellite altimetry data (1993–2016). We focus on the 74 Agulhas rings with lifetimes longer than 360 days that crossed the Walvis Ridge while moving westward. Of these 74 rings, at least three eventually reached the western boundary. For one of them, first detected at 39.5°S, 14.6°E and hereafter referred to as Ring Lilian, we present direct *in situ* measurements at the Brazilian continental slope that document its interaction with the Brazil Current, and two cyclonic eddies. While moving across the South Atlantic, this ring captured some surface drifters, and also Argo floats that sampled its vertical temperature and salinity structure. The combination of different techniques and sampling instruments provides a robust and comprehensive view of the lifetime of the Ring Lilian since its origin until the eventual demise into the Brazil Current, after a 4-year journey across the South Atlantic.

The paper is organized as follows. In Section 2, we present the eddy detection and tracking algorithm, the satellite and *in situ* data sets, as well as the method for estimate volume and energy of the rings. Section 3 summarizes the results of the ring census, and discusses the interaction of Ring Lilian with the Brazil Current. Concluding remarks are then presented at Section 4.

2. Methods

2.1. Eddy detection and tracking

An oceanic mesoscale eddy is a nonlinear rotating coherent structure with horizontal dimension scaled by the local Rossby radius of deformation. They show up on altimetry maps as closed contours of sea surface height which are parallel to stream functions in a non-divergent flow, in geostrophic approximation. That is the basis of the geometric methods which have been used to detect eddies both visually or by automated algorithms (*e.g.*, Byrne et al., 1995; Schouten et al., 2000; Chaigneau et al., 2008, 2009; Chelton et al., 2011). However, a weakness arises from the fact that geometric methods usually require a threshold that varies according to the region, what can be a problem in global assessments. Another issue is the need for a shape criterion to minimize false detections (Kurian et al., 2011; Mason et al., 2014).

A more dynamical approach is provided by the Okubo-Weiss parameter (W) that is a physical criterion to evaluate the relative importance of vorticity and deformation in a non-divergent bi-dimensional flow (Okubo, 1970; Weiss, 1991), as expressed by the equation:

$$W = S_n^2 + S_s^2 - \omega^2,$$

where normal (S_n) and shear (S_s) components of strain and vorticity (ω) are defined, respectively, as:

$$S_n = \frac{\partial u'}{\partial x} - \frac{\partial v'}{\partial y}, \quad S_s = \frac{\partial v'}{\partial x} + \frac{\partial u'}{\partial y}, \quad \omega = \frac{\partial v'}{\partial x} - \frac{\partial u'}{\partial y}.$$

The residual surface velocity field components (u',v') are calculated from the horizontal gradient of the altimetric sea level anomaly, assuming a geostrophic balance:

$$u' = -\frac{g}{f}\frac{\partial \eta}{\partial x}, \quad v' = \frac{g}{f}\frac{\partial \eta}{\partial y},$$

where η is sea level anomaly, g is gravity acceleration, f is the Coriolis parameter, and x and y are the meridional and zonal distances, respectively. A high vorticity region surrounded by high rates of strain defines a vortex and shows up on a map as closed contours of W. A threshold is recommended to improve the distinction capacity of the method (Elhmaïdi et al., 1993). Following previous works, we used a constant value $W_0 = -2\times10^{-12}$ s^{-2} (Chelton et al., 2007; Souza et al., 2011).

The Okubo-Weiss has been effective both in regional (Isern-Fontanet et al., 2003, 2004; Morrow, 2004; Henson and Thomas, 2008; Mill

et al., 2015) and global eddy coverage assessments (Chelton et al., 2007). However, some difficulties emerge from pure W fields as the second derivatives of η add numerical noise and usually create false positives (Souza et al., 2011). Chaigneau et al. (2008), in an evaluation of automated eddy detection algorithms, found that the Okubo-Weiss presents a success of detection rate of 97%, but an excess of detection rate (*i.e.*, false positives) of 76%.

A new hybrid method that matches closed contours of sea surface height and Okubo-Weiss parameter has been used to detect and track eddies on satellite altimetry maps (Halo et al., 2014; Raj et al., 2016). This approach accounts for the fact that a geostrophic eddy core is both dominated by vorticity ($W<W_0$) and enclosed within a loop of sea surface height. Our automated hybrid algorithm is a parallelized version of the original Pierrick Penven Matlab script for Simple Ocean Eddy Detection (publicly available at http://sourceforge.net/projects/eddydetect/) written in Python.

The eddy detection starts seeking for local extrema (maxima and minima) on a sea surface height field. Then, W is calculated from the geostrophic velocity and smoothed by double passing a Hanning filter to reduce the grid scale noise created by the second derivatives of η (Chelton et al., 2007, 2011). If there are closed sea surface height loops around the extremum, the eddy amplitude is determined by the difference between the extremum and the outermost closed loop circumscribed to the vorticity dominated area ($W<W_0$). Valid eddies should contain only one extremum, at least four grid points within the outermost closed loop, and radius limited to the range 40–300 km. The eddy radius is defined as the radius of a circle equivalent to the area within the outer closed loop.

The tracking process aims to identify eddies in successive time steps which represent the same eddy translating in the ocean. An m-by-n matrix $\boldsymbol{X}$, where m and n are the numbers of eddies detected at times t and $t+1$, respectively, is filled with a generalized Euclidean distance in a non-dimensional property space, taking as reference the center of the eddy, according to the following equation (Penven, 2005):

$$X_{t,t+1} = \sqrt{\left(\frac{\Delta X}{X_0}\right)^2 + \left(\frac{\Delta R}{R_0}\right)^2 + \left(\frac{\Delta \omega}{\omega_0}\right)^2}$$

where ΔX is the distance between the eddies detected at times t and $t+1$, ΔR is the variation of radius, and $\Delta\omega$ is the variation of vorticity. The denominators of the three terms represent characteristic values previously defined (respectively, $X_0 = 100$ km, $R_0 = 100$ km, and $\omega_0 = 1\times10^{-5}$ s^{-1}). The minimum matrix element $x_{i,j}$ defines an eddy match. If the geographical distance between the matched eddies implies an unrealistic speed or a swap in the vorticity polarity, the eddy at time t is considered dead, and the eddy at time $t+1$will be a newborn. If a split-off occurs, the farther eddy is designated as a newborn, while the closest holds the label of the former track. In case of merging, the algorithm continues the track of the nearest eddy from the previous time step.

2.2. Altimetry

Merged multi-mission altimeter data present better spatial and temporal resolution and lower error than mono-mission data, being more suitable for mesoscale processes analyses (Chassignet et al., 1992; Le Traon et al., 1998, 2003; Ducet et al., 2000; Pascual et al., 2006). We used daily merged SLA maps from the new DUACS DT2014, distributed on a ¼° × ¼° Cartesian grid, for the period between 1 January 1993 and 5 May 2016. This product includes data from all available altimeter missions (Jason-1&2&3, TOPEX/Poseidon, Envisat, GFO, ERS-1&2, HY-2A, Saral/Altika, Cryosat-2). The SLA is relative to a mean sea surface calculated with a 20-year altimeter reference period. For details about this dataset see Pujol et al. (2016).

2.3. In situ observations

Surface drifting buoys tracked by satellites were also used to support ring identification. Drifters captured by Agulhas rings performed anticyclonic loops, roughly following lines of the same sea surface height. The dataset from the Global Drifter Program (GDP) is quality controlled and interpolated to regular ¼-day intervals (Lumpkin and Pazos, 2007). Two Argo profilers (WMO 1900284 and WMO 1900285) sampled the Ring Lilian over the Mid-Atlantic Ridge. These floats provided temperature and salinity profiles that help to assess the vertical structure of the ring.

A mooring line deployed 150 km south of Cape Frio (23°S, 42°W), off the southeast Brazil coast, recorded the passage of the Ring Lilian. This line was equipped with an upward-looking 75 kHz Acoustic Doppler Current Profiler (ADCP) mounted at 400 m and four current meters placed at depths of 600, 800, 1200 and 1564 m. At the surface, a buoy was equipped with a single-point current meter at a depth of 1.5 m (Vogel et al., 2010). The current data were recorded at 20-min intervals from 28 April 2006 through 20 June 2008. The data series were hourly vector averaged, and a 40-h low-pass Butterworth filter was applied to remove inertial motion and tides (Roberts and Roberts, 1978).

2.4. Ring structure

We estimated the size and intensity of the rings regarding volume anomaly (*Vol*), available potential energy (*APE*) and kinetic energy (*KE*), using formulation derived from a two-layer model with reduced gravity as follows:

$$Vol = \int_A (h - h_\infty) dA,$$

$$APE = \frac{\rho g'}{2} \int_A (h - h_\infty)^2 dA,$$

$$KE = \frac{\rho}{2} \int_A h v^2 dA,$$

where h is the depth of the 10 °C isotherm within the ring, h_∞ is the depth of the 10 °C isotherm far from the ring, A is the surface area of the ring, ρ is the mean potential density of the surface layer, g' is the reduced gravity, and v is the azimuthal velocity. For details see Olson et al. (1985), Olson and Evans (1986), and Garzoli et al. (1999).

3. Results and discussion

The automated algorithm detected the shedding of 140 rings from the retroflection during ~24 years, between 1 January 1993 and 5 May 2016. The number of rings spawned per year varied between 3 and 8, yielding an average of 6.0 ± 1.2 rings/year, in agreement with the literature (*e.g.*, Lutjeharms, 1981). Out of the 140 rings, 81 demised in the Cape Basin, 49 coalesced with older rings, three were reabsorbed by the retroflection, two still were in the Cape Basin at the end of the period, and five left the basin crossing the Walvis Ridge. Most of these interactions occurred at the southeastern Cape Basin, where a regime of turbulent mixing and stirring prevails. Boebel et al. (2003) named this region “Cape Cauldron” and proposed it as a transition between the Agulhas Retroflection and the northwestern Cape Basin, where isolated Agulhas rings show up embedded in the Benguela Current. Our results show that while 140 rings spawned from the Agulhas Retroflection, their following dissipation, splitting and merging resulted in 74 long-lived rings that crossed the Walvis Ridge and translated towards the west, being five directly stemmed from the Agulhas Retroflection and 69 split-offs from Agulhas rings. The tracks fill almost entirely the Cape Basin area and the rings crossed the Walvis Ridge between 23°S and 35°S, creating a well-developed corridor across the Atlantic (Fig. 1a). Results obtained by Dencausse et al. (2010) are consistent with our findings. The authors point out the complexity of interactions of

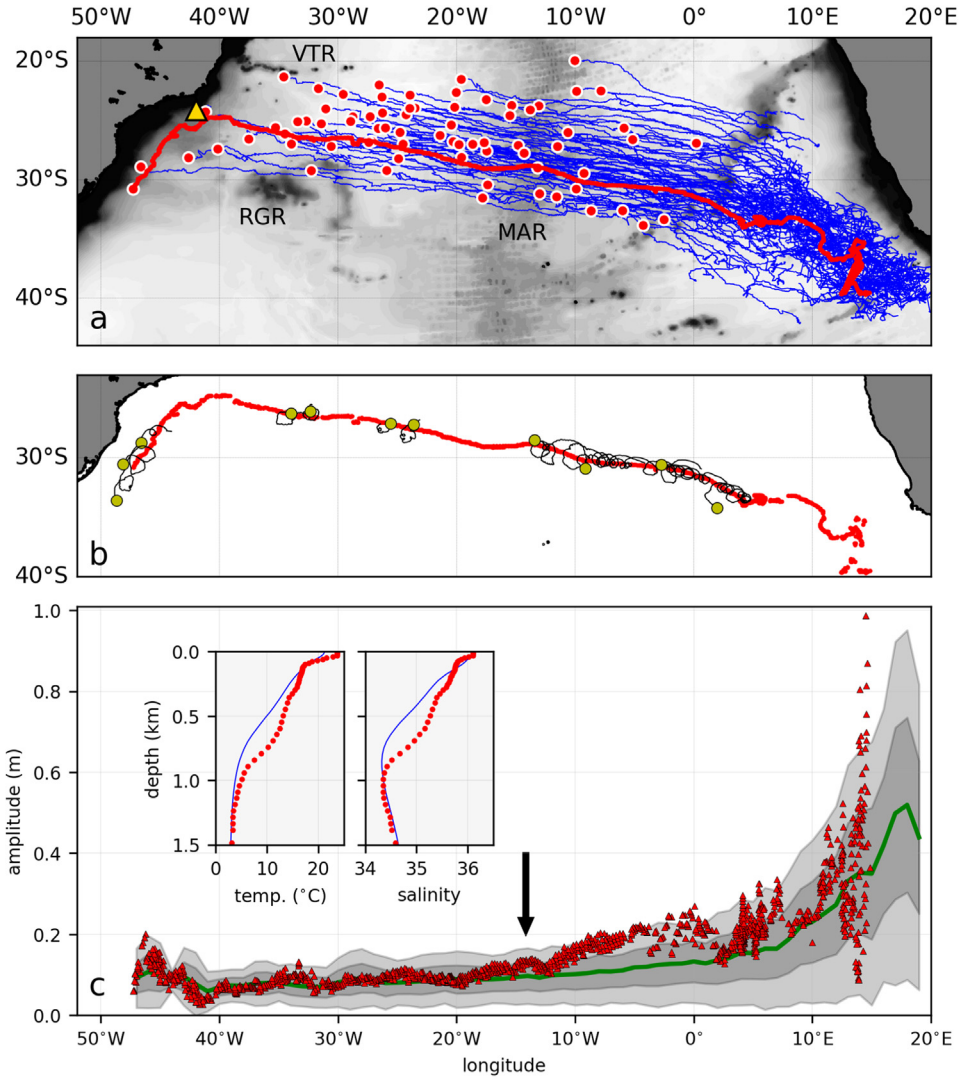

Fig. 1. Rings' tracks and decay curve. (a) Tracks of Agulhas rings since Cape Basin, from 1993 through 2016, based on altimetry data analysis with an automated detecting and tracking hybrid algorithm. Red line shows the track of the Ring Lilian from its origin until its passage by the mooring site located within the Brazil Current region (yellow triangle). The acronyms MAR, RGR, and VTR refers to Mid-Atlantic Ridge, Rio Grande Rise, and Vitória-Trindade Ridge, respectively. (b) Surface drifters performing anticyclonic loops when captured by the Ring Lilian. (c) Mean amplitude decay curve as a function of longitude for the Agulhas rings (green line). The dark gray shows one standard deviation and the light, two standard deviations. The evolution of the Ring Lilian amplitude is highlighted in red. The insets show vertical profiles of temperature and salinity (red for Argo float data and blue for climatology) measured inside the Ring Lilian at longitude 13°W (indicated by the arrow). (For interpretation of the references to color in this figure legend, the reader is referred to the web version of this article.)

Agulhas rings with bathymetry, cyclones, and other rings as a cause for splitting, merging and other transformations. They found that the minority (19%) of all Agulhas rings observed in the period 1993–2007, not only the long-lived ones, were "initial rings" (directly shed by the retroflection) that never subdivide.

Besides the vigorous eddy activity in the "Cape Cauldron", the interaction of rings with bottom topography is also a key to split-up events that may occur when rings reach the eastern flank of the Walvis Ridge and more frequently when colliding with the Vema Seamount (31°S, 9°E). When this happens, the ring can be destroyed or split off one or more eddies. The role of the Vema Seamount in ring split-up was previously documented by Arhan et al. (1999) and Schouten et al. (2000).

We counted the rings crossing the meridians 10°E, 0°W, 10°W, 20°W, 30°W, 40°W, and 45°W, and computed statistics for some of their main characteristics (Table 1). The average lifetime and traveled distance of the rings are 948 ± 259 days and 5748 ± 1464 km, respectively, including the trajectories of parent rings, in case of split-offs. The rings' decay is evident in several parameters, such as amplitude, vorticity, volume, and energy (APE and KE), as well as in the decreasing number of rings towards the west. The exponential decay observed within Cape Basin, with e-folding distance of O(1700–3000) km, is followed by a linear decay phase, in accordance with the literature (Byrne et al., 1995). Fig. 1c illustrates this behavior for amplitude. Potential and kinetic energy are higher in the so-called Cape Cauldron region, especially close to the retroflection. A notable increase of the kinetic energy occurs at the western boundary due to the interaction with the Brazil Current (Table 1). Despite the long journey across the South Atlantic, the Agulhas rings that reach the western boundary present mean APE and KE that are two to three times the energy of cyclonic rings pinched off the Brazil Current (Mill et al., 2015).

The ring diameter decays at a lower rate than the amplitude. This finding is supported by Dencausse et al. (2010) that estimated a mean initial diameter of the Agulhas rings at 240 km, decreasing to about 170 km at the longitude 10°E. Our estimate at this longitude is slightly smaller (Table 1). Nevertheless, it should be noted that while Dencausse et al. (2010) used a method based on wavelet analysis that admittedly overestimates the radius of maximum swirl velocity, ours represent the core of rings determined by $W < W_0$. As the Okubo-Weiss method allegedly underestimates the diameter of vortices (Isern-Fontanet et al., 2006; Henson and Thomas, 2008; Souza et al., 2011), we used the geostrophic surface velocity to evaluate the diameter of the maximum swirl velocity around each ring. This diameter was determined with a negligible difference to the one estimated using W (less than altimetric map resolution), endorsing the findings by Font et al. (2004).

We calculated the phase speed of the first baroclinic mode of the Rossby waves for each ring position through the entire period, using a linear, two-layer theory for free Rossby waves on a resting ocean with a flat bottom, and compared this to the respective rings' translation speeds. The histograms in Fig. 2 show that, on average, rings are faster

Table 1
Agulhas rings properties by longitude bands for the period between 1993 and 2016. Ring statistics (mean ± standard deviation) derived from the automated algorithm that identified 74 long-lived Agulhas rings leaving the Cape Basin. List of parameters: n is the number of rings that reach the meridian; Amplitude is the difference between the sea surface height in the center of the ring and at the border; Radius is the radius of a circle with area equivalent to the region circumscribed to the maximum radial velocity around the ring; Vorticity is the mean surface vorticity; Volume is that part of the ring with waters warmer than 10 °C referenced to the depth of the 10 °C isotherm in the surrounding region; APE[a] is the available potential energy; KE[b] is the kinetic energy integrated over the layer above the 10 °C isotherm.

Longitude reached by the rings	45°W	40°W	30°W	20°W	10°W	0°W	10°E
n	2	5	18	42	63	73	74
Amplitude (m)	0.11 ± 0.04	0.07 ± 0.02	0.08 ± 0.03	0.09 ± 0.04	0.10 ± 0.04	0.13 ± 0.05	0.23 ± 0.10
Radius (km)	64 ± 6	71 ± 13	80 ± 16	81 ± 12	79 ± 9	73 ± 10	77 ± 16
Vorticity (10^{-6} s^{-1})	8.42 ± 2.63	4.65 ± 0.68	3.98 ± 0.73	4.40 ± 1.01	5.16 ± 1.11	7.16 ± 1.87	9.97 ± 2.83
Volume (10^{12} m^3)	2.1 ± 0.8	1.7 ± 1.0	2.5 ± 1.6	2.9 ± 1.9	3.2 ± 1.7	3.6 ± 2.1	8.0 ± 6.7
APE (10^{15} J)	0.7 ± 0.4	0.3 ± 0.3	0.6 ± 0.5	0.8 ± 0.9	1.0 ± 0.9	1.4 ± 1.4	6.2 ± 9.2
KE (10^{15} J)	1.7 ± 1.0	0.5 ± 0.2	0.7 ± 0.5	0.7 ± 0.6	0.9 ± 0.6	1.3 ± 1.1	4.1 ± 3.8

[a] $APE = \frac{\rho g'}{2}\int_A (h - h_\infty)^2 dA$.
[b] $KE = \frac{\rho}{2}\int_A hv^2 dA$.

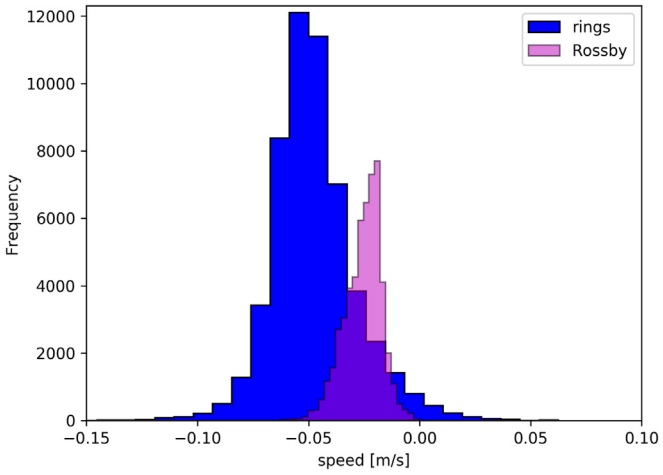

Fig. 2. Histograms of the propagation speed of the rings tracked since the Cape Basin zone and phase speed of the first-mode baroclinic Rossby waves calculated for rings positions at each day.

than Rossby waves, although there is a significant overlap. Oliveira and Polito (2013) show that the propagation speeds of waves and eddies are similar in the South Atlantic between 10°S and 35°S, while Polito and Sato (2015) reveal that 42–61% of vortices ride the Rossby waves. However, Killworth and Blundell (2005, 2004) have shown that the too simplistic model used in many studies (*e.g.*, Chelton et al., 2007; Polito and Sato, 2015) that results in faster-than-theory waves can be significantly improved towards the observed phase speeds just with the inclusion of bottom topography and a mean baroclinic flow. Therefore, the result showed in Fig. 2 should be considered with some caution.

In the Brazil Basin, after crossing the Mid-Atlantic Ridge, the rings seem to be constrained by the bathymetry of the southern flank of the Vitória-Trindade Ridge (21°S, 40–29°W) and the north of the Rio Grande Rise (30°S, 35°W), suggesting a deep-reaching characteristic (Fig. 1a). From 74 long-lived Agulhas rings tracked over more than 23 years of altimetric data, at least three of them eventually reached the western boundary. The velocity structure of one of them, the Ring Lilian, was recorded for several days by an instrumented mooring line deployed 150 km south of Cape Frio, Brazil. Its path is highlighted in red, and a yellow triangle marks the mooring site in Fig. 1a.

During the 3.5 years in which Lilian was crossing the South Atlantic, several surface drifters were entrained into the ring and performed anticyclonic loops, even when it was already embedded in the Brazil Current (Fig. 1b - drifters 39682, 34390, 40008, 44175, 39624, 41290, 60357, 44053). Two Argo floats (1900284 and 1900285) profiled the Ring Lilian eleven times over the Mid-Atlantic Ridge, at 13°W. We compared a pair of measured temperature and salinity profiles to the World Ocean Atlas 2013 seasonal climatology (Fig. 1c, insets) (Locarnini et al., 2013; Zweng et al., 2013). The water mass at intermediate depths inside the ring was warmer and saltier than climatology while Argo profiles outside the ring (not shown) were similar to climatology. These profiles show how the heat and salt transports by Agulhas rings based on the 10 °C isotherm choice may be underestimated. The maximum temperature anomaly (+5 °C) was observed approximately at 700 m depth while the maximum salinity anomaly (+0.6) was observed at approximately 600 m. Two thermostads and respective halostads were recorded inside the ring (depth of 120–280 m, temperature of 16–17 °C, and salinity of 35.6–35.7; depth of 360–600 m, temperature of 12–14 °C, and salinity of 35.1–35.3), corresponding to South Indian Subtropical Mode Water (SIMW) (Olson et al., 1992; Byrne et al., 1995) and Subantarctic Mode Water (Garzoli et al., 1999; McDonagh and Heywood, 1999), respectively. Hydrographic data obtained in the vicinity of the Agulhas Retroflection show SIMW with a characteristic 17 °C thermostad (Byrne et al., 1995) and a deeper (440–580 m) thermostad of 12.2 °C with a corresponding halostad of 35.07–35.10 (Garzoli et al., 1999). This colder thermostad is related to the injection, during the ring shedding process, of Subantarctic Surface Water south of the subtropical front near the retroflection (Arhan et al., 1999).

The amplitude decay curve is shown in the Fig. 1c. Similar decay curves for Agulhas rings have been presented in previous studies but based on SLA and not, as in our case, on ring amplitude (Byrne et al., 1995; Schouten et al., 2000). The average curve presents an exponential decay in the Cape Basin and a linear behavior beyond the Walvis Ridge. The Ring Lilian is not unusual regarding amplitude. When Ring Lilian reached the Brazil Current, its amplitude was about one-third of the value at meridian 0°W, indicating that it had lost most of its energy, since the amplitude is a proxy for APE. However, the analysis of the mooring data will show that Ring Lilian was still relatively strong, with kinetic energy comparable to that of the Brazil Current and associated cyclonic eddies, and able to impact the current velocity measured at the mooring site. The ring moved southwestward with the Brazil Current flow until 30°S, where its altimetric signal fades in the Brazil-Malvinas Confluence eddy field.

The rings tracked in this study show a well defined positive SLA signature, clearly discernible from the background. That is also the case for Ring Lilian, whose signal can be unequivocally followed since its origin both in the SLA and in the W contours. Additional material provided online shows the clear signal of Ring Lilian from its origin until approaching the western boundary. Many tracks of Agulhas rings are discernible in Chelton's global eddy-tracking dataset (Chelton et al., 2011), including Lilian (track label 147078).

Satellite-derived SLA and associated surface geostrophic velocities

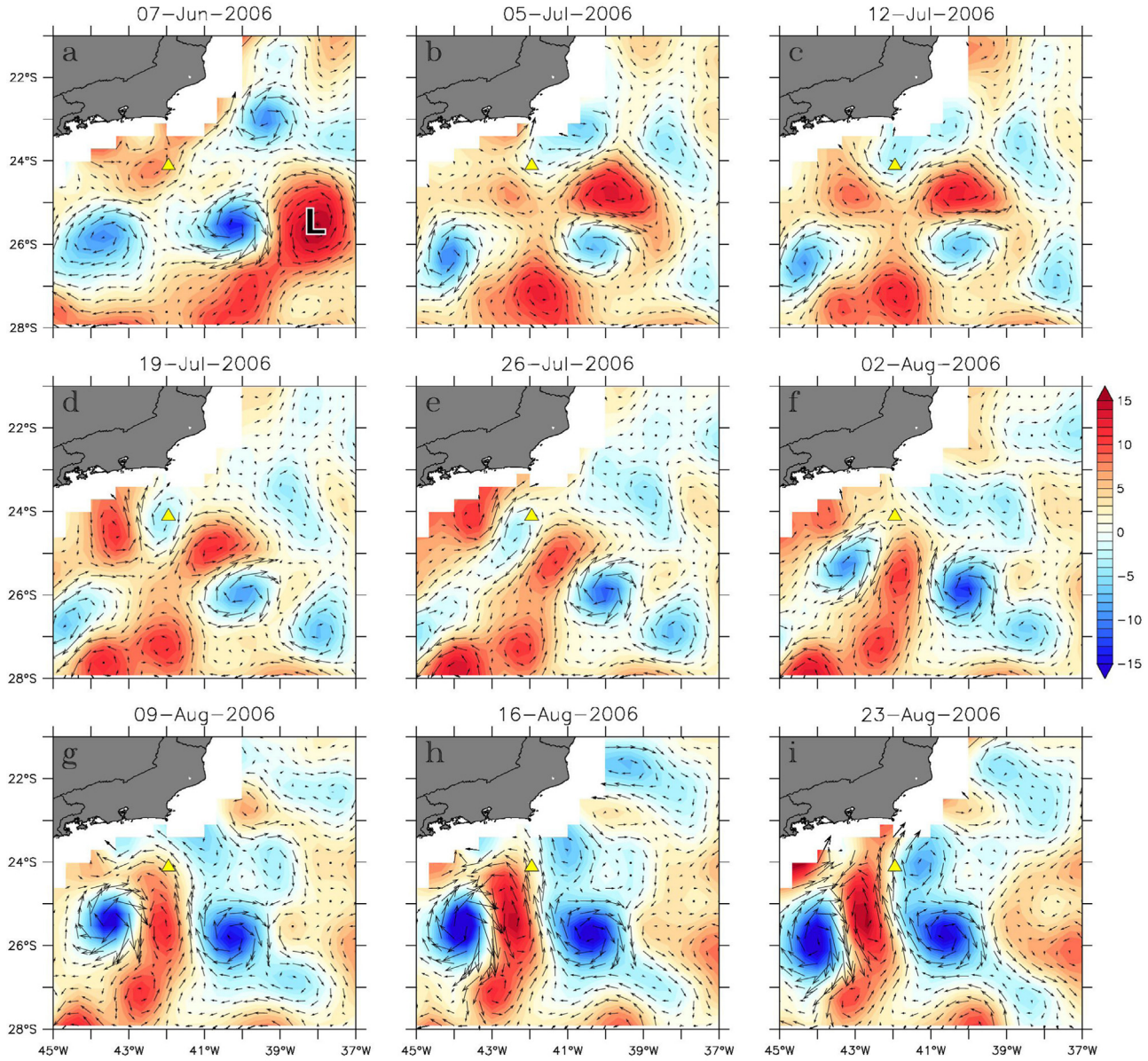

Fig. 3. Final approach of the Ring Lilian. The Ring Lilian approaching the Brazil Current and interacting with two cyclones, as seen in snapshots of SLA from satellite altimetry. Arrows show the surface geostrophic velocity anomaly. Yellow triangle marks the mooring line position. The Lilian is the positive (red) anomaly located at 25.5°S and 38°W in the upper-left panel (a), labeled with an "L", which moves northwestward toward the mooring site until 12 July, and then southwestward sandwiched between the two cyclones, or negative (blue) anomalies. (For interpretation of the references to color in this figure legend, the reader is referred to the web version of this article.)

provided a broad spatial and temporal view of the interaction between Lilian and the Brazil Current (Fig. 3). As the ring approached the mooring site, on 7 June 2006, it encountered two cyclonic eddies locally generated by the Brazil Current instability (Fig. 3a) (*e.g.*, da Silveira et al., 2008; Mano et al., 2009; Mill et al., 2015). The ring slowly moved between these two eddies, around 5 July (Fig. 3b), and the set turned in an anti-clockwise rotation and moved toward the mooring site. The northernmost cyclone, at this time still a large meander in the Brazil Current off Cape Frio, crossed the mooring site first; after almost one month, on 2 August, (Fig. 3f) the northern edge of Lilian began crossing the mooring site. Its signature, as indicated by the surface geostrophic velocities, would last for about 20 days, until 23 August (Fig. 3i), when the second cyclone, also a Cape Frio eddy that had been pinched off from the current months before, approached the mooring location. The strongest northward surface velocity anomalies induced by Ring Lilian were observed around 16 August.

This sequence of events, based on the satellite-derived SLA, is corroborated by *in situ* measurements. A unique record of ADCP velocities provides direct insight into the vertical structure of an Agulhas Ring that arrived in the Brazil Current region. The current is strongly baroclinic, with average velocities that tend to vanish at approximately 400 m (Fig. 4a). Before the arrival of Ring Lilian, the surface velocities recorded at the mooring (Fig. 4b) show a relatively stable southwestward flow until 2 August which can be associated with the Brazil Current flow. The main direction of the flow is also illustrated in Fig. 4a for the water column down to 400 m by the average zonal and meridional velocities. At the beginning of August, with the approach of the Ring Lilian, the magnitude of the flow at the mooring site suddenly decreased to almost zero, then started to increase rapidly. The current changed direction toward a more zonal flow and velocities peaked at 1.2 m/s by the middle of the month (Fig. 4b, velocity not filtered).

The strength of the Brazil Current flow makes it difficult to fully

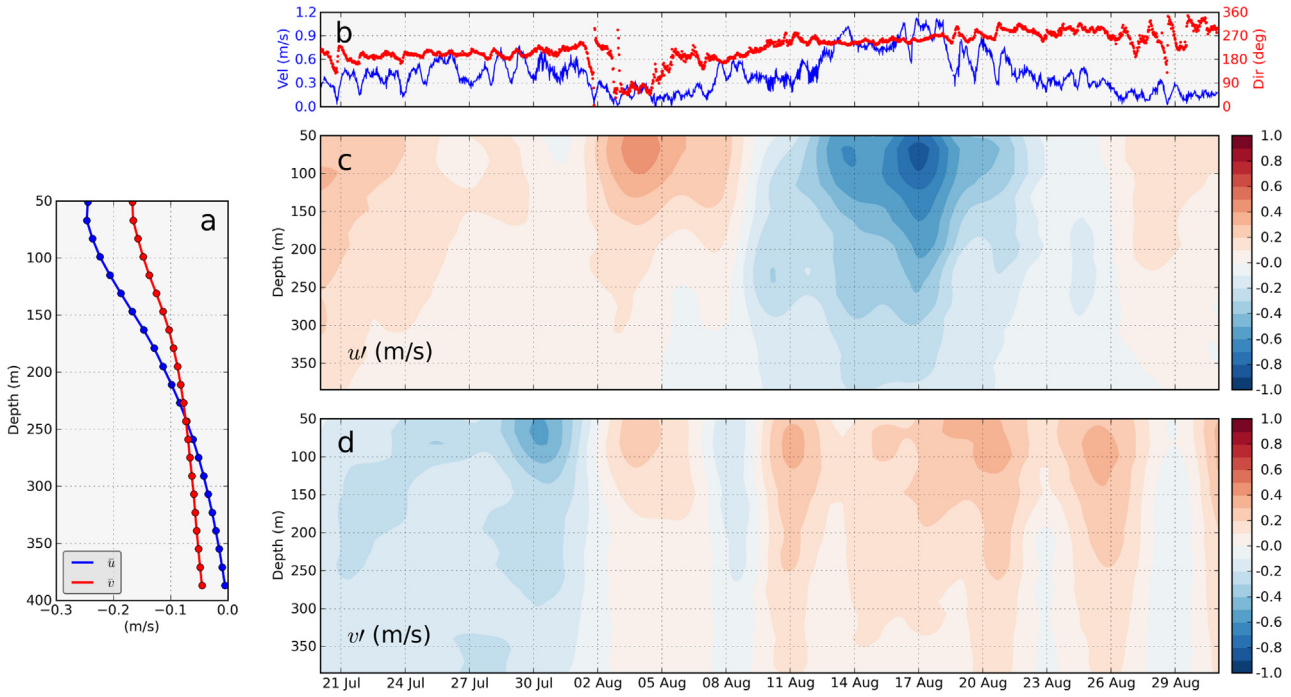

Fig. 4. Recorded velocities at the mooring site. (a) Average Brazil Current velocity profiles - blue for zonal and red for meridional velocities. (b) Time series of surface velocity magnitude (blue) and direction (red). (c) Zonal – u and (d) Meridional - v anomalous velocities - blue tones mean negative (westward and southward) anomalies and red tones positive (eastward and northward) anomalies. (For interpretation of the references to color in this figure legend, the reader is referred to the web version of this article.)

comprehend the influence of the two cyclones and Ring Lilian through the analysis of total velocities. This influence, however, can be highlighted by computing anomalous *in situ* zonal (u') and meridional (v') velocities (Fig. 4c and d) by removing the 2-year mean values. Note that in comparison with geostrophic velocity anomalies computed from the SLA, a perfect match should not be expected because of the spatial and temporal resolution of the satellite data and ageostrophic effects. The mooring data show that until the beginning of August, the influence of the northern and then the eastern edge of the first cyclone is predominant, as indicated by the positive u' and negative v'. The beginning of August marks a transition period, with positive u' and v', indicating northeastward flow, which is also suggested by the geostrophic velocities shown in Fig. 3f for this period. From 9 August onward, there is a flow inversion, beginning with negative u' and positive v' and then changing after 21 August to almost zero u' and positive v'. This flow inversion indicates the influence of the northern and then the eastern edges of the Ring Lilian over the mooring site, “sandwiched” at this point between the two cyclones (Fig. 3, lower panels).

While the velocity anomalies associated with the cyclone have a strong barotropic component, the anomalies during the passage of the Ring Lilian through the mooring site are more baroclinic. In fact, current meter velocities below 400 m (Fig. 5) show that the cyclone influence is strong until at least 800 m, and still noticeable down to 1500 m, while the signal associated with the Agulhas ring becomes weak below 400 m. It is notable, however, that its influence can still be felt at such depths after a 3.5-year lifetime and a journey of more than 5500 km.

4. Conclusions

This study documents the translation of long-lived Agulhas rings throughout the South Atlantic Ocean, based on ~24 years of altimeter data from 1993 through 2016. The rings were traced since their generation site using an automated hybrid detecting and tracking algorithm. The longer time series and the use of multi-mission satellite data provide a more robust statistics than previous studies.

A total of 140 rings were shed from the Agulhas retroflection, leading to an average of 6.0 ± 1.2 rings per year. After substantial transformation and interaction with topography and other eddies, including merging and splitting of rings, 74 rings with lifetimes longer than one year managed to cross the Walvis Ridge and propagated westward into the Atlantic, with speeds significantly higher than that of linear Rossby waves. A fast exponential decay of the ring properties within Cape Basin, such as amplitude and vorticity, is followed by a slow linear decay phase after crossing the ridge. At least for one ring, Argo floats document the transport of subsurface (16–17 °C) and intermediate (12–14 °C) modal waters well into the Atlantic.

Most rings lose their surface signature while translating in the South Atlantic Ocean, and the number of rings decays fast with longitude. Six rings, however, reached 40°W, at the vicinity of the western boundary, and three rings hit the Brazil Current south of Cape Frio (latitude 23°S, longitude 42°W). For one such ring (named Ring Lilian in this study), its interaction with the Brazil Current and with two local cyclones was recorded by a mooring line located at the Brazilian continental slope. The record shows that the local perturbation lasted for approximately one month.

Judging from its surface signature in altimetry, Ring Lilian was not a particularly strong ring, and its decay curve follows pretty much the behavior of the total set of Agulhas rings. The Argo and velocity data, however, provided a complimentary view of ring decay. According to the Argo profiles, while at 15°W Lilian still presented a deep structure, with temperature and salinity anomalies reaching down to 1200 m, next the Brazilian margin at 42°W its radial velocity signal was significant only down to 400 m. The shrinking of its vertical extension evidences the erosion of the ring along its translation. At the western boundary, however, Ring Lilian is still strong enough to significantly influence the local dynamics. While colliding with the Brazil Current and being squeezed between two locally formed cyclonic eddies, Lilian leads to an increase of the local surface velocities by a factor of three. The Brazil Current is well known as a weaker counterpart of the

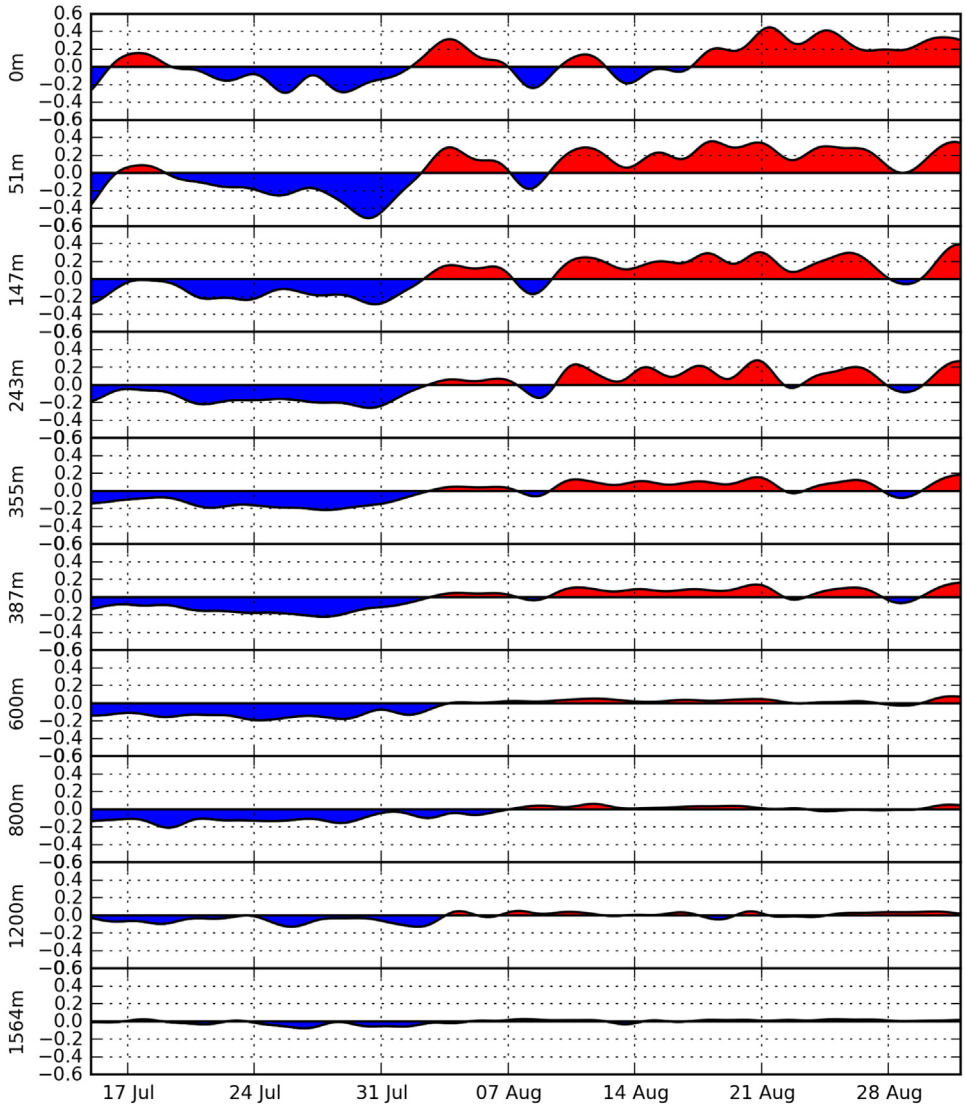

Fig. 5. Time series of anomalous meridional velocity in m/s. The record, from the surface to bottom, shows the flow inversion during the passage of the Ring Lilian. For this plot data from different instruments were used, including the surface single-point current meter, the 75 kHz ADCP, and four current meters.

generally strong western boundary currents, and the maximum recorded velocity of 1.2 m/s, associated with the tripole formed by Lilian and the two cyclones, is not easily observed in the region.

Our analysis of the altimetry data indicates that the data recorded at the mooring site may not represent a unique event and that the arrival of Agulhas rings, if not common (3 rings in ~24 years), may be recurrent and have a significant local impact. These rings represent an extra source of energy and vorticity usually neglected in regional modeling, which may have direct implications for the correct simulation of the flow variability and dynamics. The formation of an eddy tripole and its further propagation southward along the Santos Basin as a train of vorticity waves show that the interaction between an Agulhas ring and the Brazil Current may not necessarily be just that of an eddy colliding with a boundary current, as previously investigated (Azevedo et al., 2012) in a theoretical framework, but instead can be more complicated and involve other eddies. How much do the Agulhas rings effectively contribute to the mesoscale variability in that region, and how much do they represent significant energy pulses that may trigger Brazil Current transport variability, possibly feeding back into the interior of the South Atlantic domain, are still open questions that demand further investigation.

Acknowledgements

The authors thank Queiroz Galvão Exploração e Produção S.A., OGX Petróleo e Gás Participações S.A., and Barra Energia do Brasil Petróleo e Gás Ltda. for permitting the use of the mooring data in this publication. The SSALTO/DUACS altimeter products were produced and distributed by the Copernicus Marine and Environment Monitoring Service (CMEMS) (http://www.marine.copernicus.eu). The GDP surface drifter data was provided by the Atlantic Oceanographic and Meteorological Laboratory (AOML, http://www.aoml.noaa.gov/phod/dac). The Argo data were collected and made freely available by the international Argo Project (a pilot program of the Global Ocean Observing System) and contributing national programs (http://www.argo.net; http://argo.jcommops.org). This work is a contribution to the INCT-PROOCEANO, a National Institute for Science and Technology for Integrated Studies of Processes along Continental and Slope Waters supported by CNPq (National Council for Scientific and Technological Development, Brazil). EPC acknowledges NSF (National Science Foundation, USA) grant 0928271.

Appendix A. Supplementary material

Supplementary data associated with this article can be found in the online version at doi:10.1016/j.dsr.2018.08.005.

References

Arhan, M., Mercier, H., Lutjeharms, J.R.E., 1999. The disparate evolution of three Agulhas rings in the South Atlantic Ocean. J. Geophys. Res. 104, 20987–21005.

Azevedo, J.L.L., Nof, D., Mata, M.M., 2012. Eddy-train encounters with a continental boundary: a South Atlantic case study. J. Phys. Oceanogr. 42, 1548–1565.

Bang, N.D., 1970. Dynamic interpretations of a detailed surface temperature chart of the Agulhas Current Retroflexion and fragmentation area. S. Afr. Geogr. J. 52, 67–76.

Beal, L.M., De Ruijter, W.P.M., Biastoch, A., Zahn, R., 2011. SCOR/WCRP/IAPSO Working Group 136. On the role of the Agulhas system in ocean circulation and climate. Nature 472, pp. 429–436.

Beismann, J.O., Käse, R.H., Lutjeharms, J.R.E., 1999. On the influence of submarine ridges on translation and stability of Agulhas rings. J. Geophys. Res.: Oceans 104, 7897–7906.

Bennett, A.F., 1978. Poleward heat fluxes in Southern Hemisphere oceans. J. Phys. Oceanogr. 8, 785–798.

Biastoch, A., Böning, C.W., Schwarzkopf, F.U., Lutjeharms, J.R.E., 2009. Increase in Agulhas leakage due to poleward shift of Southern Hemisphere westerlies. Nature 462, 495–499.

Boebel, O., Lutjeharms, J.R.E., Schmid, C., Zenk, W., Rossby, T., Barron, C., 2003. The Cape Cauldron: a regime of turbulent inter-ocean exchange. Deep Sea Res. Part 2 Top. Stud. Oceanogr. 50, 57–86.

Byrne, D.A., Gordon, A.L., Haxby, W.F., 1995. Agulhas eddies a synoptic view using Geosat ERM data. J. Phys. Oceanogr. 25, 902–917.

Casanova-Masjoan, M., Pelegrí, J.L., Sangrà, P., Martínez, A., Grisolía-Santos, D., Pérez-Hernández, M.D., Hernández-Guerra, A., 2017. Characteristics and evolution of an Agulhas ring. J. Geophys. Res. C: Oceans 122, 7049–7065.

Chaigneau, A., Gizolme, A., Grados, C., 2008. Mesoscale eddies off Peru in altimeter records: identification algorithms and eddy spatio-temporal patterns. Prog. Oceanogr. 79, 106–119.

Chaigneau, A., Eldin, G., Dewitte, B., 2009. Eddy activity in the four major upwelling systems from satellite altimetry (1992–2007). Prog. Oceanogr. 83, 117–123.

Chassignet, E.P., Holland, W.R., Capotondi, A., 1992. Impact of the altimeter orbit on the reproduction of oceanic rings-application to a regional model of the Gulf Stream. Oceanol. Acta 15, 479–490.

Chelton, D.B., Schlax, M.G., Samelson, R.M., de Szoeke, R. a., 2007. Global observations of large oceanic eddies. Geophys. Res. Lett. 34, 1–5.

Chelton, D.B., Schlax, M.G., Samelson, R.M., 2011. Global observations of nonlinear mesoscale eddies. Prog. Oceanogr. 91, 167–216.

da Silveira, I.C.A., Lima, J.A.M., Schmidt, A.C.K., Ceccopieri, W., Sartori, A., Franscisco, C.P.F., Fontes, R.F.C., 2008. Is the meander growth in the Brazil Current system off Southeast Brazil due to baroclinic instability? Dyn. Atmos. Oceans 45, 187–207.

Dencausse, G., Arhan, M., Speich, S., 2010. Routes of Agulhas rings in the southeastern Cape Basin. Deep Sea Res. Part I 57, 1406–1421.

Ducet, N., Le Traon, P.Y., Reverdin, G., 2000. Global high-resolution mapping of ocean circulation from TOPEX/Poseidon and ERS-1 and −2. J. Geophys. Res. 105, 19477.

Duncombe Rae, C.M., 1991. Agulhas retroflection rings in the South Atlantic Ocean: an overview. S. Afr. J. Mar. Sci. 11, 327–344.

Elhmaïdi, D., Provenzale, A., Babiano, A., 1993. Elementary topology of two-dimensional turbulence from a Lagrangian viewpoint and single-particle dispersion. J. Fluid Mech. 257, 533–558.

Font, J., Isern-Fontanet, J., De Jesus Salas, J., 2004. Tracking a big anticyclonic eddy in the western Mediterranean Sea. Sci. Mar. 68, 331–342.

Fu, L.-L., Zlotnicki, V., 1989. Observing oceanic mesoscale eddies from Geosat altimetry: preliminary results. Geophys. Res. Lett. 16, 457–460.

Garnier, E., Verron, J., Barnier, B., 2003. Variability of the South Atlantic upper ocean circulation: a data assimilation experiment with 5 years of TOPEX/POSEIDON altimeter observations. Int. J. Remote Sens. 24, 911–934.

Garzoli, S.L., Gordon, A.L., 1996. Origins and variability of the Benguela Current. J. Geophys. Res. 101, 897–906.

Garzoli, S.L., Richardson, P.L., Duncombe Rae, C.M., Fratantoni, D.M., Goñi, G.J., Roubicek, A.J., 1999. Three Agulhas rings observed during the Benguela Current Experiment. J. Geophys. Res. 104, 20971–20985.

Garzoli, S.L., Baringer, M.O., Dong, S., Perez, R.C., Yao, Q., 2013. South Atlantic meridional fluxes. Deep Sea Res. Part I 71, 21–32.

Goni, G.J., Garzoli, S.L., Roubicek, A.J., Olson, D.B., Brown, O.B., 1997. Agulhas ring dynamics from TOPEX/Poseidon satellite altimeter data. J. Mar. Res. 55, 861–883.

Gordon, A.L., 1985. Indian-Atlantic transfer of thermocline water at Agulhas retroflection. Science 227, 1030–1033.

Gordon, A.L., 1986. Interocean exchange of thermocline water. J. Geophys. Res. 91, 5037–5046.

Gordon, A.L., Haxby, W.F., 1990. Agulhas eddies invade the South Atlantic: Evidence from Geosat altimeter and shipboard conductivity-temperature-depth survey. J. Geophys. Res. C: Oceans 95, 3117–3125.

Gordon, A.L., Weiss, R.F., Smethie Jr., W.M., Warner, M.J., 1992. Thermocline and Intermediate Water communication between the South Atlantic and Indian Oceans. J. Geophys. Res. 97, 7223–7240.

Gründlingh, M.L., 1995. Tracking eddies in the southeast Atlantic and southwest Indian oceans with TOPEX/POSEIDON. J. Geophys. Res. 100, 24977–24986.

Halo, I., Backeberg, B., Penven, P., Ansorge, I., Reason, C., Ullgren, J.E., 2014. Eddy properties in the Mozambique channel: a comparison between observations and two numerical ocean circulation models. Deep Sea Res. Part 2 Top. Stud. Oceanogr. 100, 38–53.

Hastenrath, S., 1982. On meridional heat transport in the world ocean. J. Phys. Oceanogr. 12, 922–927.

Henson, S.A., Thomas, A.C., 2008. A census of oceanic anticyclonic eddies in the Gulf of Alaska. Deep Sea Res. Part I 55, 163–176.

Isern-Fontanet, J., García-Ladona, E., Font, J., 2003. Identification of Marine Eddies from Altimetric maps. J. Atmos. Ocean. Technol. 20, 772–778.

Isern-Fontanet, J., Font, J., García-Ladona, E., Emelianov, M., Millot, C., Taupier-Letage, I., 2004. Spatial structure of anticyclonic eddies in the Algerian basin (Mediterranean Sea) analyzed using the Okubo–Weiss parameter. Deep Sea Res. Part 2 Top. Stud. Oceanogr. 51, 3009–3028.

Isern-Fontanet, J., García-Ladona, E., Font, J., 2006. Vortices of the Mediterranean sea: an Altimetric perspective. J. Phys. Oceanogr. 36, 87–103.

Kamenkovich, V.M., Leonov, Y.P., Nechaev, D.A., 1996. On the influence of bottom topography on the Agulhas Eddy. J. Phys. Oceanogr. 26, 892–912.

Killworth, P.D., Blundell, J.R., 2004. The dispersion relation for planetary waves in the presence of mean flow and topography. Part I: analytical theory and one-dimensional examples. J. Phys. Oceanogr. 34, 2692–2711.

Killworth, P.D., Blundell, J.R., 2005. The dispersion relation for planetary waves in the presence of mean flow and topography. Part II: two-dimensional examples and global results. J. Phys. Oceanogr. 35, 2110–2133.

Kurian, J., Colas, F., Capet, X., McWilliams, J.C., 2011. Eddy properties in the California current system. J. Geophys. Res. 116.

Le Bars, D., Durgadoo, J.V., Dijkstra, H.A., Biastoch, A., De Ruijter, W.P.M., 2014. An observed 20-year time series of Agulhas leakage. Ocean Sci. 10, 601–609.

Le Traon, P.-Y., Nadal, F., Ducet, N., 1998. An improved mapping method of multisatellite altimeter data. J. Atmos. Ocean. Technol. 15, 522–534.

Le Traon, P.-Y., Faugère, Y., Hernandez, F., Dorandeu, J., Mertz, F., Ablain, M., 2003. Can we merge GEOSAT follow-on with TOPEX/Poseidon and ERS-2 for an improved description of the ocean circulation? J. Atmos. Ocean. Technol. 20, 889–895.

Locarnini, R.A., Mishonov, A.V., Antonov, J.I., Boyer, T.P., Garcia, H.E., Baranova, O.K., Zweng, M.M., Paver, C.R., Reagan, J.R., Johnson, D.R., et al., 2013. World Ocean Atlas 2013, volume 1: temperature. In: NOAA Atlas NESDIS. NOAA, Silver Spring, MD, pp. 73.

Lumpkin, R., Pazos, M., 2007. Measuring surface currents with surface velocity program drifters: the instrument, its data, and some recent results. In: Lagrangian Analysis and Prediction of Coastal and Ocean Dynamics. Cambridge University Press, New York, NY, pp. 39–67.

Lutjeharms, J.R.E., 1981. Spatial scales and intensities of circulation in the ocean areas adjacents to South Africa. Deep-Sea Res. 28A, 1289–1302.

Lutjeharms, J.R.E., 1996. The exchange of water between the South Indian and South Atlantic Oceans. In: Wefer, G., Berger, W.H., Siedler, G., Webb, D.J. (Eds.), The South Atlantic - Present and Past Circulation. Springer-Verlag, Berlin Heidelberg, pp. 125–162.

Lutjeharms, J.R.E., Cooper, J., 1996. Interbasin leakage through Agulhas current filaments. Deep-Sea Res. I 43, 213–238.

Lutjeharms, J.R.E., Gordon, A.L., 1987. Shedding of an Agulhas ring observed at sea. Nature 325, 138–140.

Lutjeharms, J.R.E., Van Ballegooyen, R.C., 1988a. The retroflection of the Agulhas current. J. Phys. Oceanogr. 18, 1570–1583.

Lutjeharms, J.R.E., Van Ballegooyen, R.C., 1988b. Anomalous upstream retroflection in the Agulhas current. Science 240, 1770–1772.

Mano, M.F., Paiva, A.M., Torres, A.R., Coutinho, A.L.G.A., 2009. Energy flux to a cyclonic Eddy off Cabo Frio, Brazil. J. Phys. Oceanogr. 39, 2999–3010.

Mason, E., Pascual, A., McWilliams, J.C., 2014. A new sea surface height–based code for oceanic mesoscale eddy tracking. J. Atmos. Ocean. Technol. 31, 1181–1188.

Matano, R.P., Beier, E.J., 2003. A kinematic analysis of the Indian/Atlantic interocean exchange. Deep Sea Res. Part 2 Top. Stud. Oceanogr. 50, 229–249.

McCartney, M.S., Woodgate-Jones, M.E., 1991. A deep-reaching anticyclonic eddy in the subtropical gyre of the eastern South Atlantic. Deep-Sea Res. 38, S411–S443.

McDonagh, E.L., Heywood, K.J., 1999. The origin of an anomalous ring in the Southeast Atlantic. J. Phys. Oceanogr. 29, 2050–2064.

McDonagh, E.L., King, B.A., 2005. Oceanic fluxes in the South Atlantic. J. Phys. Oceanogr. 35, 109–122.

Mey, R.D., Walker, N.D., Jury, M.R., 1990. Surface heat fluxes and marine boundary layer modification in the Agulhas Retroflection region. J. Geophys. Res. 95, 15997–16015.

Mill, G.N., da Costa, V.S., Lima, N.D., Gabioux, M., Guerra, L.A.A., Paiva, A.M., 2015. Northward migration of Cape São Tomé rings, Brazil. Cont. Shelf Res. 106, 27–37.

Morrow, R., 2004. Divergent pathways of cyclonic and anti-cyclonic ocean eddies. Geophys. Res. Lett. 31, 1–5.

Nof, D., 1999. Strange encounters of eddies with walls. J. Mar. Res. 57, 739–761.

Nof, D., Zharkov, V., Ortiz, J., Paldor, N., Arruda, W., Chassignet, E.P., 2011. The arrested Agulhas retroflection. J. Mar. Res. 69, 659–691.

Okubo, A., 1970. Horizontal dispersion of floatable particles in the vicinity of velocity singularities such as convergences. Deep Sea Res. Oceanogr. Abstr. 17, 445–454.

Oliveira, F.S.C., Polito, P.S., 2013. Characterization of westward propagating signals in the South Atlantic from altimeter and radiometer records. Remote Sens. Environ. 134, 367–376.

Olson, D.B., Evans, R.H., 1986. Rings of the Agulhas Current. Deep-Sea Res. 33, 27–42.

Olson, D.B., Schmitt, R.W., Kennelly, M., Joyce, T.M., 1985. A two-layer diagnostic model of the long-term physical evolution of warm-core ring 82B. J. Geophys. Res. 90, 8813–8822.

Olson, D.B., Fine, R.A., Gordon, A.L., 1992. Convective modifications of water masses in

the Agulhas. Deep-Sea Res. 39, S163–S181.
Pascual, A., Fauge, Y., Larnicol, G., Le Traon, P.-Y., 2006. Improved description of the ocean mesoscale variability by combining four satellite altimeters. Geophys. Res. Lett. 33, 1–4.
Penven, P., 2005. Average circulation, seasonal cycle, and mesoscale dynamics of the Peru Current System: a modeling approach. J. Geophys. Res. 110, 1736.
Polito, P.S., Sato, O.T., 2015. Do eddies ride on Rossby waves? J. Geophys. Res. C: Oceans 120, 5417–5435.
Pujol, M.-I., Faugère, Y., Taburet, G., Dupuy, S., Pelloquin, C., Ablain, M., Picot, N., 2016. DUACS DT2014: the new multi-mission altimeter data set reprocessed over 20 years. Ocean Sci. 12.
Raj, R.P., Johannessen, J.A., Eldevik, T., Nilsen, J.E.Ø., Halo, I., 2016. Quantifying mesoscale eddies in the Lofoten Basin. J. Geophys. Res. C: Oceans 121, 4503–4521.
Roberts, J., Roberts, T.D., 1978. Use of the Butterworth low-pass filter for oceanographic data. J. Geophys. Res. 83, 5510.
de Ruijter, W.P.M., Boudra, D.B., 1985. The wind-driven circulation in the South Atlantic-Indian Ocean—I. Numerical experiments in a one-layer model. Deep Sea Res. A 32, 557–574.
de Ruijter, W.P.M., Biastoch, A., Drijfhout, S.S., Lutjeharms, J.R.E., Matano, R.P., Pichevin, T., van Leeuwen, P.J., Weijer, W., 1999. Indian-Atlantic interocean exchange: dynamics, estimation and impact. J. Geophys. Res. 104, 20885–20910.
Schouten, M.W., De Ruijter, W.P.M., Van Leeuwen, P.J., Lutjeharms, J.R.E., 2000. Translation, decay and splitting of Agulhas rings in the southeastern Atlantic Ocean. J. Geophys. Res. 105, 21913–21925.
Souza, J.M.A.C., de Boyer Montégut, C., Le Traon, P.-Y.,, 2011. Comparison between three implementations of automatic identification algorithms for the quantification and characterization of mesoscale eddies in the South Atlantic Ocean. Ocean Sci. 7, 317–334.
van Aken, H.M., van Veldhoven, A.K., Veth, C., de Ruijter, W.P.M., van Leeuwen, P.J., Drijfhout, S.S., Whittle, C.P., Rouault, M., 2003. Observations of a young Agulhas ring, Astrid, during MARE in March 2000. Deep Sea Res. Part 2 Top. Stud. Oceanogr. 50, 167–195.
van Ballegooyen, R.C., Gründlingh, M.L., Lutjeharms, J.R.E., 1994. Eddy fluxes of heat and salt from the southwest Indian Ocean into the southeast Atlantic Ocean: a case study. J. Geophys. Res. 99, 14053–14070.
van Sebille, E., Barron, C.N., Biastoch, A., van Leeuwen, P.J., Vossepoel, F.C., de Ruijter, W.P.M., 2009. Relating Agulhas leakage to the Agulhas Current retroflection location. Ocean Sci. 5, 511–521.
Vogel, M., Silveira, I.C.A., Castro, B.M., Lima, J.A.M., Pereira, A.F., Williams, P., 2010. Metocean Measurements at Northern Santos Basin-Brazil, In: Proceedings of the Offshore Technology Conference. Offshore Technology Conference, Houston, TX, p. OTC 20947.
Weijer, W., De Ruijter, W.P.M., Sterl, A., Drijfhout, S.S., 2002. Response of the Atlantic overturning circulation to South Atlantic sources of buoyancy. Glob. Planet. Change 34, 293–311.
Weiss, J., 1991. The dynamics of enstrophy transfer in two-dimensional hydrodynamics. Phys. D 48, 273–294.
Witter, D.L., Gordon, A.L., 1999. Interannual variability of South Atlantic circulation from four years of TOPEX/Poseidon satellite altimeter observations. J. Geophys. Res. 104, 20927–20948.
Wunsch, C., Heimbach, P., 2013. Two decades of the Atlantic meridional overturning circulation: anatomy, variations, extremes, prediction, and overcoming its limitations. J. Clim. 26, 7167–7186.
Zweng, M.M., Reagan, J.R., Antonov, J.I., Locarnini, R.A., Mishonov, A.V., Boyer, T.P., Garcia, H.E., Baranova, O.K., Johnson, D.R., Seidov, D., 2013. Others. World ocean atlas 2013. Volume 2, Salinity.